

# Layer-Wise Data-Free CNN Compression

Maxwell Horton  
Apple

mhorton@apple.com

Yanzi Jin  
Apple

yanzi\_jin@apple.com

Ali Farhadi  
Apple

afarhadi@apple.com

Mohammad Rastegari  
Apple

mrastegari@apple.com

## Abstract

*We present an efficient method for compressing a trained neural network without using any data. Our data-free method requires 14x-450x fewer FLOPs than comparable state-of-the-art methods [6, 51]. We break the problem of data-free network compression into a number of independent layer-wise compressions. We show how to efficiently generate layer-wise training data, and how to precondition the network to maintain accuracy during layer-wise compression. We show state-of-the-art performance on MobileNetV1 [24] for data-free low-bit-width quantization. We also show state-of-the-art performance on data-free pruning of EfficientNet B0 [46] when combining our method with end-to-end generative methods.*

## 1. Introduction

Inference with Convolutional Neural Networks (CNNs) is typically computationally expensive [24, 22, 42, 41]. As a result, practical methods for compressing CNNs are of great interest. Application domains involving machine learning on low-power, low-compute devices require efficient CNNs for on-device execution. Examples include smart-home security, factory automation, and mobile applications. One common technique for improving CNN computational efficiency is weight pruning [29, 47, 18, 13]. The removal of network weights allows the network to occupy a smaller memory footprint and achieve a faster execution time. Another common technique for improving a CNN’s runtime efficiency is quantization. In many cases, a CNN with 32-bit weights and activations can be converted to a CNN with a lower-bit representation (e.g. 8-bit, 4-bit, or even 1-bit) with little or no loss of accuracy [27, 38, 26].

Most methods for CNN compression require retraining on the original training set to achieve a high compression rate. For example, compressing through sparsity [29, 47, 18, 13] requires training on the original data. Applying post-training quantization usually results in poor network accuracy [26] unless special care is taken in adjusting network weights [38]. Handling low-bit quantization

provides additional challenges when data is not available. Unfortunately, many real-world scenarios require compression of an existing model but prohibit access to the original dataset. For example, data which is legally sensitive, or which has privacy restrictions, may not be easily accessible. In some cases, data may not be available if a model which has already been deployed needs to be compressed.

We propose a simple and efficient method for achieving high compression rates for data-free network compression. Our method is a layer-wise optimization based on the teacher-student paradigm [23]. A pretrained model is used as a teacher that will help train a compressed student model. During optimization, we generate data to approximate the input to a layer of the teacher network and use it to optimize the corresponding layer in the compressed student network. Figure 1 illustrates an overview of our method. This layer-wise optimization approach allows us to converge faster while still maintaining high accuracy, resulting in a significantly more efficient compression process than end-to-end network optimization [15, 51].

Our method can be integrated with any compression scheme for the student network. In this paper, we show how weight pruning and network quantization can be used. We precondition the network to bring weights across layers to a similar scale, then we use BatchNorm [25] statistics to generate data used for layer-wise pruning and quantization. Our method is 14x-450x more efficient than comparable generative methods. We achieve state-of-the-art results for data-free quantization of MobileNets [24] on the challenging ImageNet [9] dataset. We also combine our method with generative methods to achieve state-of-the-art in data-free pruning of EfficientNet B0 [46] on ImageNet [9].

## 2. Related Work

**Pruning and Quantization:** Soft Threshold Reparameterization (STR) [29] achieves state-of-the-art results with a simple training technique that encourages increasing levels of sparsity as training progresses. Several other works present magnitude-based pruning methods [18, 47, 19, 16, 3, 39]. Alternatives to magnitude-based pruning involve using gradient information [13, 30, 21, 10, 8], covariance in-

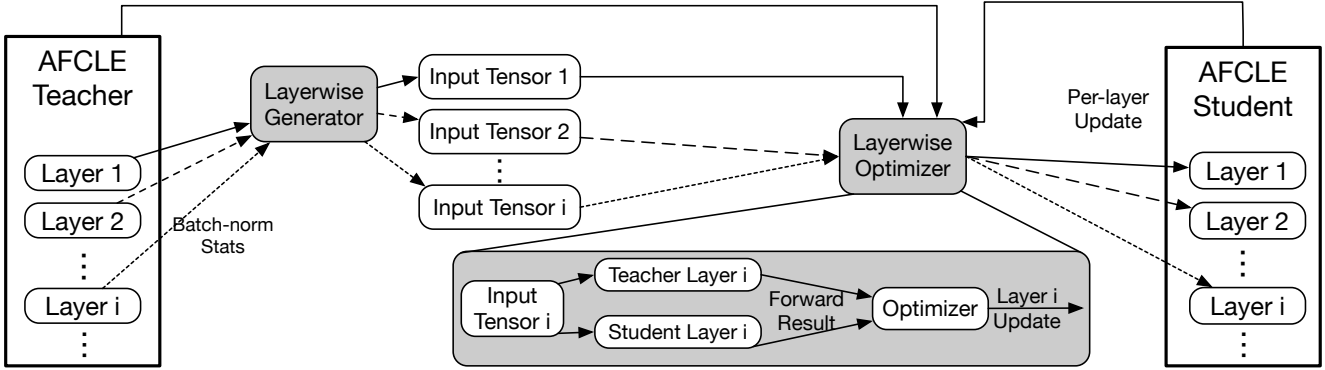


Figure 1. An overview of our method. We first perform BatchNorm fusion and Assumption-Free Cross-Layer Equalization (AFCLE, Section 3.2) on the teacher and student. Then, we train each layer of the student separately. We generate data using BatchNorm statistics from the previous layer (Section 3.1), then use this data to optimize the compressed student network to match the teacher.

formation [32], or regularization [34]. Refer to [29] for a more comprehensive overview.

Quantization involves reducing the numerical precision of weights and/or activations from a typical 32-bit floating point representation to a lower-bit integral representation [27, 17, 33, 14, 31]. Methods typically quantize between 8 bits [48, 4, 26, 27, 50] and 1 bit [41, 7, 11, 35]. The most commonly used quantization scheme is affine quantization [26]. Other formulations can include a scale and a zero-point for each output channel [27].

**Data-Light and Data-Free Compression:** A few recent works have explored methods for quantizing a model using little data (“data-light” methods) or no data (“data-free” methods). In the data-light method, AdaRound [37], the authors devise a method for optimizing the rounding choices made when quantizing a weight matrix. In the data-free method Data-Free Quantization Through Weight Equalization and Bias Correction (DFQ) [38], the authors manipulate network weights and biases to reduce the post-training quantization error. Other network equalization methods tackle the problem of data-free quantization, such as Weight Factorization [36].

A few works have explored data-light and data-free pruning. In the data-light method, Principle Filter Analysis [45], activation correlations are used to prune filters. An iterative data-free pruning method is presented in Data-Free Parameter Pruning [44], though they only prune fully-connected layers. Optimal Brain Damage [8] presents results for data-light and data-free pruning for overparameterized networks such as AlexNet [28]. The data-light method Optimal Brain Surgeon [21] uses second-order derivatives, and related layer-wise methods exist [12].

**Generative Methods for Data-Free Compression:** Given a trained model, it’s possible to create synthetic images that match characteristics of the training set’s statistics. These images can be used to retrain a more efficient model using only another pretrained model. These methods are

computationally expensive.

In Deep Inversion (DI) [51], the authors use a pretrained model to generate a dataset used to train a sparse model. To generate the dataset, a noise image is trained to match the network’s BatchNorm [25] statistics, and to look realistic. The authors generate a dataset and use it to train a sparse model using Knowledge Distillation [23]. A similar method appears in The Knowledge Within [20], although their method is data-light rather than data-free.

In Adversarial Knowledge Distillation (AKD) [6], the authors generate synthetic images for model retraining using a Generative Adversarial Network (GAN) [15]. These images are used in conjunction with Knowledge Distillation [23] to train a new network. Other GAN-based formulations include Generative Low-bitwidth Data Free Quantization [49].

### 3. Layer-Wise Data-Free Compression

Our method for data-free network compression begins with a fully trained network and creates a compressed network of the same architecture. This method is conceptually similar to Knowledge Distillation [23] in that a pretrained “teacher” network is used to train a “student” network. However, Knowledge Distillation requires training data. Previous approaches have addressed this through generating data, as in Adversarial Knowledge Distillation (AKD) [6] and Deep Inversion (DI) [51]. However, these methods are computationally expensive.

We take a simpler approach illustrated in Figure 1. We view each layer of the student as a compressed approximation of the corresponding layer in the teacher. As long as the approximation of each layer is accurate, the overall student network will produce similar outputs to the teacher. This approach is far more computationally efficient than other generative methods, since our method does not need to train an input image to produce good training signal at every layer of a network. Instead, we generate inputs separately

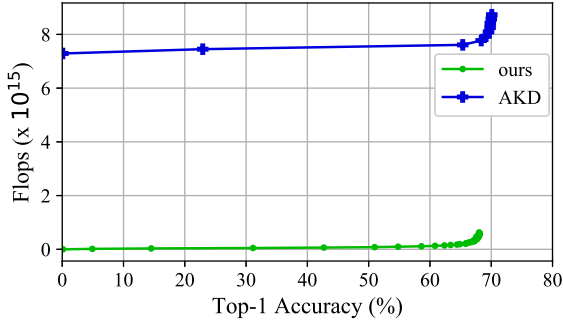


Figure 2. MobileNetV1 analysis of the number of forward-pass FLOPs and training accuracy for our method and Adversarial Knowledge Distillation (AKD) [6]. Deep Inversion [51] (not shown) takes even more FLOPs than AKD, and is less accurate.

for each individual layer, which does not require generating realistic images. Our method takes 14x fewer FLOPs than AKD [6] and 450x fewer FLOPs than DI [51] (Figure 2), converging after only a few hundred iterations.

Our first challenge lies in generating data used to train compressed approximations of the teacher’s layers. Our second challenge lies in preconditioning the network to achieve more effective compression. We address these in the following subsections.

### 3.1. Layer-Wise Data Generation

We describe our method for generating layer-wise network inputs. We assume the network is composed of blocks containing a convolution, followed by a BatchNorm [25], followed by an activation. Let  $\mathcal{B}_i$  denote the BatchNorm layer associated with a block of index  $i$ . The BatchNorm  $\mathcal{B}_i$  normalizes by the mean  $\mu_{\mathcal{B}_i}$  and standard deviation  $\sigma_{\mathcal{B}_i}$  of its inputs, then applies a channelwise affine transformation with weight  $\gamma_{\mathcal{B}_i}$  and bias  $\beta_{\mathcal{B}_i}$ . Therefore, we know that the standard deviation of the BatchNorm’s output channels is  $\gamma_{\mathcal{B}_i}$ , and the mean of the output channels is  $\beta_{\mathcal{B}_i}$ .

We exploit this information to generate layer-wise inputs. Let  $\mathcal{C}_i$  denote the convolutional layer in block  $i$  of the network, and  $f_i$  denote the activation in block  $i$ . Furthermore, let  $h(\cdot)$  denote the application of layer  $h$  to an input.

Consider the case in which block  $i$  accepts multiple input tensors from blocks indexed by a collection  $\mathcal{K}$ . Let  $x_{\mathcal{B}_{i-1}}$  denote the input into the BatchNorm  $\mathcal{B}_{i-1}$  from a training batch when training with real data. Assuming these tensors are combined by an addition function (as in Residual Networks [22]), the input  $x_{\mathcal{C}_i}$  to convolution  $\mathcal{C}_i$  is

$$x_{\mathcal{C}_i} = \sum_{j \in \mathcal{K}} f_j(\mathcal{B}_j(x_{\mathcal{B}_j})). \quad (1)$$

The extension to other combination functions besides addition is straightforward.

When training without data, we do not have access to  $x_{\mathcal{B}_j}$ , so we estimate it. Let  $\mathcal{G}_{\mathcal{C}_i}(\cdot)$  be a function that generates an input used to train layer  $\mathcal{C}_i$ . Using our observation above regarding the output statistics of BatchNorm layers, we estimate

$$x_{\mathcal{B}_j} \sim \mathcal{N}(\mu_{\mathcal{B}_j}, \sigma_{\mathcal{B}_j}) \quad (2)$$

$$\mathcal{G}_{\mathcal{C}_i} = \sum_{j \in \mathcal{K}} f_j(\mathcal{N}(\mu_{\mathcal{B}_j}, \sigma_{\mathcal{B}_j})), \quad (3)$$

where  $\mathcal{N}(\mu, \sigma)$  denotes a Gaussian function with mean  $\mu$  and standard deviation  $\sigma$ . In the case of the first convolutional layer, we generate data from  $\mathcal{N}(0, 1)$ . We ignore the effect of other layers (such as Average Pooling) on statistics.

We describe how to use this generated data to compute the student network’s layers in Section 3.3 and Section 3.4. But first, we describe another component of our method designed to precondition the network to improve final results.

### 3.2. Assumption-Free Cross-Layer Equalization

We describe our method for equalizing network layers. For ease of notation,  $W \in \mathbb{R}^{c_o, c_i}$  denotes a matrix with  $c_o$  output dimensions and  $c_i$  input dimensions. The extension of our method to convolutions is straight forward.

Our method breaks the problem of data-free network compression into the subproblem of compressing individual layers. Two issues complicate the matter of assembling a compressed network from compressed individual layers.

The first issue relates to BatchNorm [25] layers. A BatchNorm layer consists of the parameters  $\mu$ ,  $\sigma$ ,  $\gamma$ , and  $\beta$ , which correspond to the mean of its inputs, the standard deviation of its inputs, the weight of its affine transformation, and the bias of its affine transformation. Given a linear layer  $W$  with bias  $b$ , the output of the linear layer, followed by BatchNorm, is

$$f(x) = \frac{Wx + b - \mu}{\sqrt{\sigma^2 + \epsilon}} \odot \gamma + \beta, \quad (4)$$

where  $\epsilon$  is a small number used to avoid division by 0, and  $\odot$  denotes elementwise multiplication [25, 40]. If some row  $c$  of  $W$  is multiplied by a scale factor  $a$ , and if the  $c^{th}$  elements of  $b$  and  $\mu$  are multiplied by  $a$ , and if the  $c^{th}$  element of  $\gamma$  is multiplied by the scalar factor  $1/a$ , the function  $f(x)$  remains unchanged.

Thus, the relative importance of the weights of  $W$  depends on the values of BatchNorm parameters. This is problematic when pruning or quantizing  $W$  because we want the weight values’ magnitudes to reflect their importance. Hidden scale factors inside BatchNorm layers prevent this. To address this, we fuse the BatchNorm parameters  $\mu$ ,  $\sigma$ ,  $\gamma$ , and  $\beta$  into the preceding linear layer, so that the BatchNorm parameters’ effective influence on weight magnitudes is accounted for. Once this fusion occurs, BatchNorms can be

ignored. The BatchNorm statistics used in Equation 3 must be collected before this fusion step. They will remain valid, since the change in BatchNorm parameters is compensated for by the change in  $W$  and  $b$ .

The second complication with breaking data-free network compression into layer-wise compression subproblems is that the relative magnitude of weights may not be consistent across layers. Consider the output of a pair of linear layers with weights  $W_1$  and  $W_2$ , and biases  $b_1$  and  $b_2$ . Suppose the network uses ReLU activations [1], such that the output of the pair of layers is

$$f(x) = \text{ReLU}(W_1(\text{ReLU}(W_2x + b_2)) + b_1). \quad (5)$$

If row  $c$  of  $W_2$  is multiplied by a scale factor  $a$ , and if the corresponding  $c^{\text{th}}$  element of  $b_2$  is multiplied by  $a$ , and if the corresponding column  $c$  of  $W_1$  is multiplied by  $1/a$ , then output  $f(x)$  remains unchanged. In other words, the relative importance of weights across layers is not consistent a priori. This inconsistency in weight scales is problematic for layer-wise magnitude-based pruning because weights with similar importance need to have similar values across the network, or some layers will be pruned too heavily and some will not be pruned enough. The inconsistency also results in suboptimal quantization ranges, as described in [38].

To address this scaling inconsistency, we employ a method we call Assumption-Free Cross-Layer Equalization (AFCLE), which is an extension of the Cross-Layer Equalization method described in DFQ [38]. With each linear layer  $\mathcal{L}_j$  with weight  $W_j \in \mathbb{R}^{c_o \times c_i}$  and bias  $b_j \in \mathbb{R}^{c_o}$ , we associate a pair of vectors,  $v_j^i \in \mathbb{R}^{c_j}$  and  $v_j^o \in \mathbb{R}^{c_o}$ . (The extension to convolutional layers is straightforward.) These vectors will be used during AFCLE, then will remain fixed afterwards. We compute the output of our linear layer as

$$\mathcal{L}_j(x) = (W_j(x \odot v_j^i) + b_j) \odot v_j^o. \quad (6)$$

Before AFCLE, each element of the vectors  $v_j^i$  and  $v_j^o$  is initialized to 1. Consider a row  $c$  of  $W_2$  with weights  $W_2^c$ , and a corresponding column  $c$  of  $W_1$  with weights  $W_1^c$ . We calculate a scale factor  $s_c$ , and update the network as

$$s_c = \frac{\sqrt{\max(|W_1^c|) \max(|W_2^c|)}}{\max(|W_2^c|)} \quad (7)$$

$$W_1^c = W_1^c / s_c \quad (8)$$

$$v_1^o = v_1^o * s_c \quad (9)$$

$$b_1 = b_1 / s_c \quad (10)$$

$$W_2^c = W_2^c * s_c \quad (11)$$

$$v_2^i = v_2^i / s_c. \quad (12)$$

Essentially, each  $v_j^i$  and  $v_j^o$  act as a buffer that records the changes to  $W_i$  and  $b_j$ , so that we can equalize  $W_j$  across

layers without changing the network’s outputs at any layer. We iterate over all channels and over all pairs of adjacent layers in the network, regardless of whether there is a skip connection between them. We continue until the mean of all the scale parameters  $s_c$  for one round of equalization deviates from 1 by less than  $\epsilon = .001$ .

The main difference between our method and Cross-Layer Equalization (CLE) [38] is, our method uses  $v_j^i$  and  $v_j^o$  to record weight updates. CLE assumes that the updates to  $W_1^c$  and  $W_2^c$  do not alter the network, and does not include  $v_j^i$  or  $v_j^o$  terms. This assumption holds if the network’s activation functions are piecewise linear (e.g. ReLU), and if the pair of layers have no skip connections in between.

AFCLE results in no real increase in parameter count, since the vectors  $v_j^i$  and  $v_j^o$  can be folded into  $W_j$  and  $b_j$  after data-free compression is completed. The advantages of AFCLE over CLE are (1) it can be used for activation functions that aren’t piecewise linear, (2) it does not require special handling for skip connections (since any pair of layers can be equalized), and (3) it does not corrupt the Batch-Norm [25] statistics needed for data generation.

### 3.3. Data-Free Pruning

We show how to use our method to construct a sparse student without any training data. We begin by recording the BatchNorm statistics required for layer-wise data generation, as described in Section 3.1. We then perform fusion and AFCLE as a preprocessing step, as described in Section 3.2. We duplicate the resulting model to obtain a “teacher” and a “student”. For the remainder of our method, the teacher will remain unchanged, and the student will be pruned through data-free training.

We prune using Soft Threshold Reparameterization (STR) [29], which we review briefly. In the network’s convolutional and fully-connected layers, an intermediate weight  $W_s$  is calculated as

$$W_s = \text{sign}(W) \cdot \text{ReLU}(|W| - \text{sigmoid}(s)), \quad (13)$$

where  $W$  is the weight tensor, and  $s$  is a model parameter used to control sparsity. This intermediate tensor  $W_s$  is used in place of  $W$  in the forward and pass. In the backward pass, the gradients are propagated to the original weight matrix  $W$ . A weight decay parameter  $\lambda$  is used to drive  $s$  upwards from an initial value  $s_0 < 0$ , which increases sparsity.

Let  $i$  be an index assigned to the convolutional or fully-connected layer  $\mathcal{C}_i^s$  in the student model, and let the corresponding layer in the teacher model (of the same architecture) be  $\mathcal{C}_i^t$ . Let  $\mathcal{C}_i^s(\cdot)$  denote the application of layer  $s_i$  to an input tensor, and likewise for  $\mathcal{C}_i^t(\cdot)$ . Given a loss function  $L_i$  associated with layer  $i$ , we compute the loss for layer  $i$  as

$$L = L_i(\mathcal{C}_i^s(x), \mathcal{C}_i^t(x)), \quad (14)$$

where  $x \sim \mathcal{G}_{C_i^t}$  is generated from the expression in Equation 3. In our experiments, we choose  $L_i$  to be the mean square error loss for each  $i$ . We also freeze the student’s bias during training, since our goal is to induce sparsity in the weights.

### 3.4. Data-Free Quantization

The most common approach to data-free quantization of weight tensors involves examining the weight tensors, and setting the minimum and maximum quantization ranges using the minimum and maximum weight values [26]. Setting the quantized activation ranges is done in DFQ [38] by setting the maximum and minimum activation range to six standard deviations away from the mean, as determined by BatchNorm [25] statistics. The lower activation range is then clamped to 0, since ReLU [1] activations are used in their networks.

We observe that calculating the quantization ranges using these methods can suffer from outliers. The presence of a large weight or activation (whose precise value may not need to be preserved) will result in a larger quantization range, which means that smaller values will be less accurately represented by the quantization scheme. We argue that we should choose the maximum and minimum quantization range that minimize the reconstruction error of the floating-point weights or activations.

We begin our method by applying the fusion and AFCLE methods described above. Our quantization method doesn’t require backpropagation, so we do not need separate teacher and student networks. So, we refer to this network as the student, and optimize directly over its parameters.

We apply the bias absorption described in [38] to the student, to reduce biases with extremely high values. We update the BatchNorm [25] statistics needed for Equation 3 when doing so. To quantize the student’s weights, we handle each weight layer separately. We perform a simple grid search over the two quantization parameters of interest, the minimum and maximum of the quantization range. Recall that the quantized version of a floating-point tensor  $W$  can be expressed as

$$W_q = \left\lfloor \frac{\min(\max(W, l), h) - l}{k} \right\rfloor k + l, \quad (15)$$

where  $l$  is the minimum of the quantization range,  $h$  is the maximum,  $k$  is the scale factor, and  $\lfloor \cdot \rfloor$  denotes rounding to the nearest integer. As is customary, we fix

$$k = \frac{h - l}{2^n - 1}, \quad (16)$$

where  $n$  is the number of bits in the quantization scheme. Then, we perform a grid search jointly over  $h$  and  $l$  at even intervals between their minimum and maximum theoretically possible values,  $\min(W)$  and  $\max(W)$ . We find that

100 steps for each parameter is enough. We choose the  $h$  and  $l$  parameters that minimize the squared error between  $W_q$  and  $W$ .

To choose quantization parameters for our activations, we again handle each layer separately. Recall that a typical model is built from blocks consisting of a quantized convolution, followed by a BatchNorm [25], followed by an activation function, followed by a quantization module whose purpose is to quantize the activations. We want to generate data to set the minimum and maximum of the quantization range used by this quantization module.

First, we need to generate data over which to optimize our quantization module’s parameters. As in our pruning experiments, we use the generation function in Equation 3. We generate a batch of input data to the quantization module. The result is a floating-point tensor representative of the activation values that we want to quantize. We choose the minimum and maximum of the quantization range by performing the same optimization as above for weight matrices, optimizing the parameters to minimize the quantization error of the activations. Again, we find 100 iterations of grid search for each of the two parameters provides good results. If a ReLU activation is used, we clamp the lower range to 0, as in DFQ [38].

After setting the activation ranges, we run the bias correction step described in [38] to correct errors in biases introduced by quantization, taking care to update the BatchNorm [25] statistics needed in Equation 3. Then, we perform the optimization over activation ranges once more to account for the small changes in BatchNorm statistics during the bias correction step.

## 4. Experiments

We provide results for data-free pruning and quantization experiments on a variety of network architectures. We first show the results of our method compared to other computationally-efficient methods. We demonstrate that our method outperforms our baselines for providing rapid, data-free pruning.

Next, we compare our methods to computationally expensive methods requiring orders of magnitude more FLOPs. We provide an analysis of the computational efficiency of our method compared to more computationally expensive generative models. For MobileNetV1 [24] architectures, we show that our method approaches or exceeds performance of these methods. For EfficientNet [46], we show an extension of our method that combines the benefits of generative methods with our method to achieve state-of-the-art accuracy for data-free pruning.

Finally, we present results showing state-of-the-art data-free quantization using our methods. We compare to a variety of data-free methods, including generative methods, as well as methods that don’t require backpropagation.

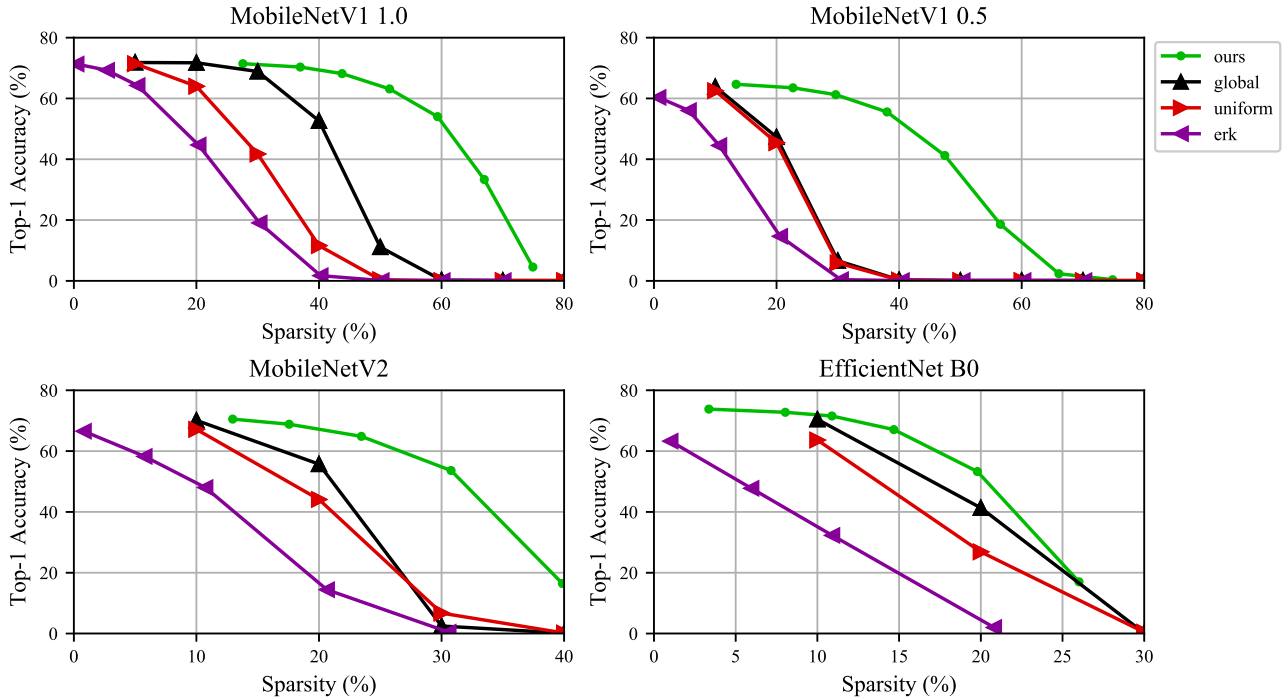


Figure 3. Comparison of our pruning method to our baselines. (Global [5]): a global magnitude threshold is used to prune weights. (Uniform [5]): a uniform layer-wise sparsity budget is used. (ERK [13]): a layer-wise sparsity budget weighted to prune more weights from larger convolutional layers, as described in Equation 17.

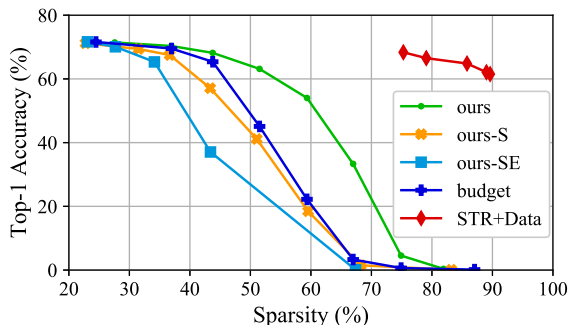


Figure 4. Ablation study of our method on MobileNetV1 1.0. (Ours-S): our method, but using data generated from  $\mathcal{N}(0, 1)$ , rather than from BatchNorm statistics. (Ours-SE): our method, with data generated from  $\mathcal{N}(0, 1)$ , and without AFCLE. (Budget): a model using the layer-wise budget learned by our method, but without training the weights. (STR+Data): the performance of Soft Threshold Reparameterization with data, as reported in [29]. This is an upper bound on performance.

In all experiments, our teacher and student network weights are initialized to a pretrained model. We train in PyTorch [40] using NVIDIA Tesla V100 GPUs. When training with our layer-wise method for pruning experiments, we train with Adam using a cosine learning rate with batch size 128. To induce sparsity in models, we used STR [29]. We

vary the  $s_0$  value (which controls initial sparsity) between  $-2$  and  $-7$ . We fix the sparsity-inducing weight decay parameter to  $\lambda = 0.00001551757813$ , as in [29].

In all MobileNetV2 [43] experiments, we replace ReLU6 with ReLU [1] as in DFQ [38]. The accuracy of this modified network is identical to that of the original MobileNetV2. When running our Assumption-Free Cross-Layer Equalization method, we don't equalize across residual connections in MobileNetV2, as in DFQ [38]. We iterate over all adjacent pairs of layers with other networks, regardless of whether skip connections are present.

When reloading pretrained networks, our floating-point accuracies for our networks were 71.82% for MobileNetV1 1.0 [24], 64.95% for MobileNetV1 0.5 [24], 71.88% for MobileNetV2 [43], and 76.30% for EfficientNet B0 [46].

#### 4.1. Efficient Data-Free Pruning Methods

We present our results for the pruning method described in Section 3.3. We empirically found that including the activations  $f_j$  in Equation 3 is not important during pruning, so we omit them from data generation for simplicity. We present results for our method in Figure 3. We compare against three baselines. The "global" baseline corresponds to applying a global threshold to a pretrained network, pruning every weight whose magnitude is smaller than the given threshold [5]. The "uniform" baseline corresponds to apply-

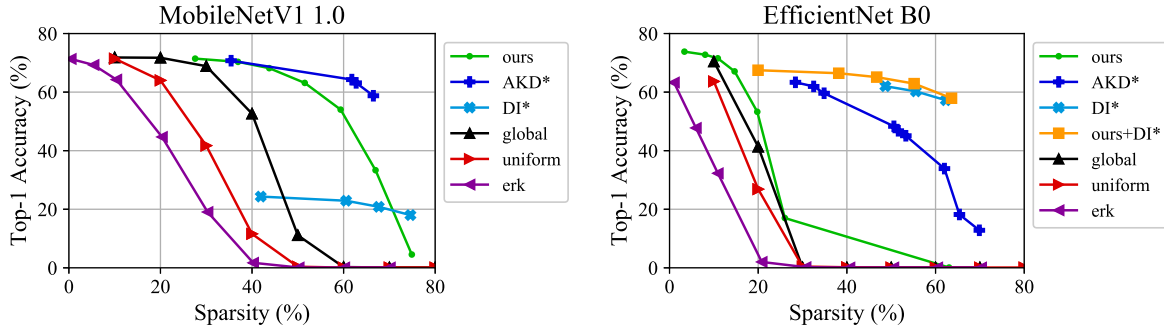


Figure 5. Performance of our method, compared to the computationally expensive methods Adversarial Knowledge Distillation (AKD) [6] and Deep Inversion (DI) [51], marked with an asterisk to denote greater computational burden. We achieve state-of-the-art accuracy for EfficientNet B0 by combining our layer-wise training method with DeepInversion.

ing a uniform sparsity level to each layer in the network by pruning the weights with smallest magnitude in each layer [5]. The Erdosh-Renyi Kernel (ERK) baseline corresponds to a budgeted layer-wise pruning suggested in RigL [13]. Each layer’s number of pruned weights is proportional to

$$p = \frac{c_o + c_i + k_h + k_w}{c_o * c_i * k_h * k_w}, \quad (17)$$

where  $c_o$  is the number of output dimensions,  $c_i$  is the number of input dimensions, and  $k_h, k_w$  are the kernel height and width.

Our method outperforms our baselines for achieving efficient, data-free sparsity. In Figure 4, we show a few ablations. We plot the accuracy of the full Soft Threshold Reparameterization [29] method when data is used (STR+Data) to estimate an upper bound on the performance of data-free pruning. We show the performance of our method without using BatchNorm [25] statistics to scale the inputs to each layer (ours-S). We instead generate data from  $\mathcal{N}(0, 1)$ . We also study the performance without scaling and without AF-CLE (ours-SE). Finally, we want to understand whether our method is simply learning an effective layer-wise budget, or whether our method is adjusting the unpruned weights to compensate for the removal of pruned weights. To investigate this, we take the final sparse models from the “ours” curve, and record their layer-wise sparsity levels. We then initialize a fresh copy of the student network, reload its pre-trained weights, and prune the smallest-magnitude weights from each layer to match the sparsity budget recorded for that layer. This result is shown as “budget” in Figure 4. Due to the lowered performance, we conclude that the optimization does more than simply learn a layer-wise sparsity budget. The optimization also adjusts network weights to compensate for pruned weights.

## 4.2. Computationally Expensive Data-Free Pruning

We present results comparing our method to more computationally expensive methods, Adversarial Knowledge

Distillation (AKD) [6] and Deep Inversion (DI) [51]. These methods involve generating end-to-end training data.

When generating data with DI [51], we use the parameters for MobileNetV2 [43] from the public GitHub repository, due to MobileNetV2’s similarities with our architectures. These settings generated images that could be recognized by an independent CNN as belonging to the given class. As in [51], we generate 165,000 images and use them to retrain a student network from a teacher network. We initialize both the student and the teacher to the same pre-trained network. We then train the student with STR [29] to match the teacher using the Label Refinery [2] formulation for Knowledge Distillation [23].

When training with AKD [6], we use the parameter settings described in [6]. We adjusted batch sizes to fit in a single NVIDIA Tesla V100 for all experiments. Again, we initialized the student and teacher networks to the same pre-trained model, then trained to induce sparsity. We also broadened our sweep of the sparsity-inducing hyperparameter  $\lambda$  (see STR [29] for details). In addition to training with  $\lambda = 0.00001551757813$ , we used values of  $2\lambda$ ,  $10\lambda$ , and  $100\lambda$  to achieve a richer variety of points on the sparsity/accuracy trade-off curve.

Results are shown in Figure 5. For brevity, we show MobileNetV1 [24] and EfficientNetB0 [46], as MobileNet V1 0.5 and MobileNetV2 [43] both had similar results to MobileNetV1. For MobileNetV1, AKD [6] outperforms our method. We emphasize that this method is 14x more computationally expensive than our method (see Figure 2). Note that DI requires 450x as much forward-pass computation as our method, and the generation phase alone takes  $1.93 \cdot 10^{17}$  forward-pass FLOPs.

For EfficientNet B0 [46], we found that DI [51] outperformed our method and AKD [6]. EfficientNet B0 contains more complicated modules than MobileNetV1 [24], including squeeze-and-excite layers and skip connections. These modules make layer-wise methods less effective, because our layer-wise loss does not accurately model the effect of these modules on accuracy when weights are pruned.

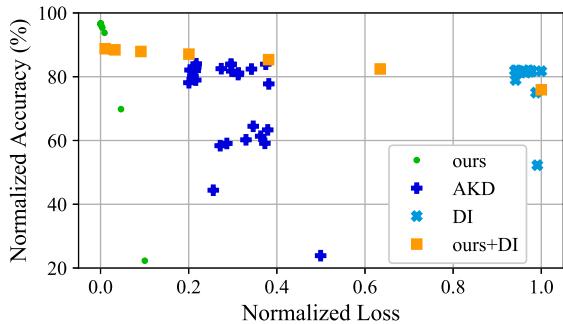


Figure 6. Correlation between normalized loss and normalized accuracy for EfficientNet B0. We find that our method demonstrates a tight correlation between loss and accuracy, even when used in conjunction with Deep Inversion, which normally does not have a tight correlation.

We found that we could improve upon the results obtained through DI [51] by applying our method in conjunction with it (“ours+DI” in Figure 5). After the forward pass of Label Refinery [2], we compute a layer-wise loss with generated data as per our method, then we perform backpropagation. We experimented with different weightings of the two losses, but found that the unweighted version performed well.

We also investigate the correlation between the loss function and the accuracy of methods for EfficientNet B0 [46]. This correlation is of particular interest in data-free retraining, because it’s plausible that in some scenarios a validation set would not be available. In this case, we may need to judge the relative quality of a variety of models by examining their loss values.

In Figure 6, we compare the loss and accuracies of our method, DI [51], AKD [6], and “ours+DI” (described above). For ease of visualization, we normalize the losses to fall in [0, 1]. We normalize model accuracies by the accuracy of the original EfficientNet B0 [46] model from which we reloaded our weights. We find that our method, as well as “ours+DI”, has a loss that is correlated with accuracy. This correlation opens the possibility for determining which of two models is superior without needing an evaluation set. The correlation between loss and accuracy is less clear for AKD and DI.

#### 4.2.1 Data-Free Quantization

We evaluate the results of our data-free quantization experiments on MobileNetV1 [24]. We compare our method to a variety of state-of-the-art data-free methods in Table 1. Note that, as described in Section 4.2.1, our method does not require backpropagation. We compare to DFQ [38], of which our method is an extension. We compare also to AdaRound [37], but with a slight modification. The original

Bits	ours	DFQ	AKD	DI
<b>MobileNetV1 1.0</b>				
8	71.11	<b>71.18</b>	70.31	24.77
7	<b>70.19</b>	69.76	68.16	25.00
6	<b>67.46</b>	61.81	61.38	19.24
5	<b>53.72</b>	25.61	31.59	9.06
4	<b>18.41</b>	0.24	0.10	0.10
<b>MobileNetV1 0.5</b>				
8	63.54	<b>63.65</b>	63.28	27.98
7	<b>61.62</b>	60.47	60.11	27.10
6	<b>55.52</b>	44.67	52.16	22.58
5	<b>30.39</b>	7.29	21.18	6.70
4	<b>3.25</b>	0.24	0.10	0.10

Table 1. Results for quantization experiments on MobileNetV1. (DFQ): Data-Free Quantization [38]. (AKD): Adversarial Knowledge Distillation [6]. (DI): Deep Inversion [51]. Note that DFQ, like our method, requires no backpropagation. AKD and DI are computationally expensive, as explained in Figure 2.

method requires using data to collect activation statistics. To compare with data-free methods, we instead generate batches of data using the BatchNorm [25] statistics of the previous layer. We also compare to the more computationally expensive generative methods Adversarial Knowledge Distillation (AKD) [6] and Deep Inversion (DI) [51]. For each method, we reload both the teacher and the student from a pretrained model.

We find that our method outperforms other methods at a variety of compression rates. In particular, for low-bit compression, our optimization over quantization ranges results in performance gains relative to the other methods. Of the methods compared, only AKD [6] and DI [51] provide a training signal that can influence the activation ranges of the weight and activation tensors. As in pruning, DI could not model the inputs to MobileNetV1 [24] well enough to achieve strong results.

## 5. Conclusion

We present a simple and effective method for data-free compression. Our method breaks this problem into the sub-problem of compressing individual layers without data. We apply a novel equalization scheme to layers to precondition networks to better maintain accuracy during compression. Then, we compress individual layers using data generated from BatchNorm [25] statistics from previous layers. Our method produces state-of-the-art results for pruning and quantization of modern architectures evaluated on ImageNet [9]. Our method is 14x-450x more efficient than state-of-the-art generative models, while maintaining competitive accuracy. Our method can also be combined with generative models to produce a new state-of-the-art in data-free compression accuracy.



## References

- [1] Raman Arora, Amitabh Basu, Poorya Mianjy, and Anirbit Mukherjee. Understanding deep neural networks with rectified linear units. *CoRR*, abs/1611.01491, 2016. 4, 5, 6
- [2] Hessam Bagherinezhad, Maxwell Horton, Mohammad Rastegari, and Ali Farhadi. Label refinery: Improving imagenet classification through label progression. *CoRR*, abs/1805.02641, 2018. 7, 8
- [3] Guillaume Bellec, David Kappel, Wolfgang Maass, and Robert Legenstein. Deep rewiring: Training very sparse deep networks, 2018. 1
- [4] Aishwarya Bhandare, Vamsi Sripathi, Deepthi Karkada, Vivek Menon, Sun Choi, Kushal Datta, and Vikram Sale-tore. Efficient 8-bit quantization of transformer neural machine language translation model, 2019. 2
- [5] Davis Blalock, Jose Javier Gonzalez Ortiz, Jonathan Frankle, and John Guttag. What is the state of neural network pruning?, 2020. 6, 7
- [6] Yoojin Choi, Jihwan Choi, Mostafa El-Khamy, and Jungwon Lee. Data-free network quantization with adversarial knowledge distillation, 2020. 1, 2, 3, 7, 8
- [7] Matthieu Courbariaux and Yoshua Bengio. Binarynet: Training deep neural networks with weights and activations constrained to +1 or -1. *CoRR*, abs/1602.02830, 2016. 2
- [8] Yann Le Cun, John S. Denker, and Sara A. Solla. Optimal brain damage. In *Advances in Neural Information Processing Systems*, pages 598–605. Morgan Kaufmann, 1990. 1, 2
- [9] J. Deng, W. Dong, R. Socher, L.-J. Li, K. Li, and L. Fei-Fei. ImageNet: A Large-Scale Hierarchical Image Database. In *CVPR09*, 2009. 1, 8
- [10] Tim Dettmers and Luke Zettlemoyer. Sparse networks from scratch: Faster training without losing performance, 2019. 1
- [11] Giuseppe Di Guglielmo, Javier Mauricio Duarte, Philip Harris, Duc Hoang, Sergio Jindariani, Edward Kreinar, Mia Liu, Vladimir Loncar, Jennifer Ngadiuba, Kevin Pedro, and et al. Compressing deep neural networks on fpgas to binary and ternary precision with hls4ml. *Machine Learning: Science and Technology*, Jun 2020. 2
- [12] Xin Dong, Shangyu Chen, and Sinno Jialin Pan. Learning to prune deep neural networks via layer-wise optimal brain surgeon. *CoRR*, abs/1705.07565, 2017. 2
- [13] Utku Evci, Trevor Gale, Jacob Menick, Pablo Samuel Castro, and Erich Elsen. Rigging the lottery: Making all tickets winners. *CoRR*, abs/1911.11134, 2019. 1, 6, 7
- [14] Ruihao Gong, Xianglong Liu, Shenghu Jiang, Tianxiang Li, Peng Hu, Jiazhen Lin, Fengwei Yu, and Junjie Yan. Differentiable soft quantization: Bridging full-precision and low-bit neural networks. In *Proceedings of the IEEE/CVF International Conference on Computer Vision (ICCV)*, October 2019. 2
- [15] Ian J. Goodfellow, Jean Pouget-Abadie, Mehdi Mirza, Bing Xu, David Warde-Farley, Sherjil Ozair, Aaron Courville, and Yoshua Bengio. Generative adversarial networks, 2014. 1, 2
- [16] Yiwen Guo, Anbang Yao, and Yurong Chen. Dynamic network surgery for efficient dnns, 2016. 1
- [17] Hai Victor Habi, Roy H. Jennings, and Arnon Netzer. Hmq: Hardware friendly mixed precision quantization block for cnns, 2020. 2
- [18] Song Han, Jeff Pool, John Tran, and William J. Dally. Learning both weights and connections for efficient neural networks. *CoRR*, abs/1506.02626, 2015. 1
- [19] Song Han, Jeff Pool, John Tran, and William J. Dally. Learning both weights and connections for efficient neural networks, 2015. 1
- [20] Matan Haroush, Itay Hubara, Elad Hoffer, and Daniel Soudry. The knowledge within: Methods for data-free model compression. *CoRR*, abs/1912.01274, 2019. 2
- [21] Babak Hassibi, David Stork, and Gregory Wolff. Optimal brain surgeon: Extensions and performance comparisons. In J. Cowan, G. Tesauro, and J. Alspector, editors, *Advances in Neural Information Processing Systems*, volume 6, pages 263–270. Morgan-Kaufmann, 1994. 1, 2
- [22] Kaiming He, Xiangyu Zhang, Shaoqing Ren, and Jian Sun. Deep residual learning for image recognition. In *Proceedings of the IEEE Conference on Computer Vision and Pattern Recognition (CVPR)*, June 2016. 1, 3
- [23] Geoffrey Hinton, Oriol Vinyals, and Jeffrey Dean. Distilling the knowledge in a neural network. In *NIPS Deep Learning and Representation Learning Workshop*, 2015. 1, 2, 7
- [24] Andrew G. Howard, Menglong Zhu, Bo Chen, Dmitry Kalenichenko, Weijun Wang, Tobias Weyand, Marco Andreetto, and Hartwig Adam. Mobilenets: Efficient convolutional neural networks for mobile vision applications. *CoRR*, abs/1704.04861, 2017. 1, 5, 6, 7, 8
- [25] Sergey Ioffe and Christian Szegedy. Batch normalization: Accelerating deep network training by reducing internal covariate shift. volume 37 of *Proceedings of Machine Learning Research*, pages 448–456, Lille, France, 07–09 Jul 2015. PMLR. 1, 2, 3, 4, 5, 7, 8
- [26] Benoit Jacob, Skirmantas Kligys, Bo Chen, Menglong Zhu, Matthew Tang, Andrew Howard, Hartwig Adam, and Dmitry Kalenichenko. Quantization and training of neural networks for efficient integer-arithmetic-only inference. In *Proceedings of the IEEE Conference on Computer Vision and Pattern Recognition (CVPR)*, June 2018. 1, 2, 5
- [27] Raghuraman Krishnamoorthi. Quantizing deep convolutional networks for efficient inference: A whitepaper. *CoRR*, abs/1806.08342, 2018. 1, 2
- [28] Alex Krizhevsky, Ilya Sutskever, and Geoffrey E Hinton. Imagenet classification with deep convolutional neural networks. In *Advances in neural information processing systems*, pages 1097–1105, 2012. 2
- [29] Aditya Kusupati, Vivek Ramanujan, Raghav Somani, Mitchell Wortsman, Prateek Jain, Sham Kakade, and Ali Farhadi. Soft threshold weight reparameterization for learnable sparsity. In *Proceedings of the International Conference on Machine Learning*, July 2020. 1, 2, 4, 6, 7
- [30] Namhoon Lee, Thalaiyasingam Ajanthan, and Philip H. S. Torr. Snip: Single-shot network pruning based on connection sensitivity, 2019. 1
- [31] R. Li, Y. Wang, F. Liang, H. Qin, J. Yan, and R. Fan. Fully quantized network for object detection. In *2019 IEEE/CVF*

- Conference on Computer Vision and Pattern Recognition (CVPR)*, pages 2805–2814, 2019. 2
- [32] Mingbao Lin, Rongrong Ji, Shaojie Li, Qixiang Ye, Yonghong Tian, Jianzhuang Liu, and Qi Tian. Filter sketch for network pruning, 2020. 2
- [33] Bin Liu, Yue Cao, Mingsheng Long, Jianmin Wang, and Jingdong Wang. Deep triplet quantization, 2019. 2
- [34] Christos Louizos, Max Welling, and Diederik P. Kingma. Learning sparse neural networks through  $l_0$  regularization, 2018. 2
- [35] Brais Martinez, Jing Yang, Adrian Bulat, and Georgios Tzimiropoulos. Training binary neural networks with real-to-binary convolutions, 2020. 2
- [36] Eldad Meller, Alexander Finkelstein, Uri Almog, and Mark Grobman. Same, same but different - recovering neural network quantization error through weight factorization. *CoRR*, abs/1902.01917, 2019. 2
- [37] Markus Nagel, Rana Ali Amjad, Mart van Baalen, Christos Louizos, and Tijmen Blankevoort. Up or down? adaptive rounding for post-training quantization, 2020. 2, 8
- [38] Markus Nagel, Mart van Baalen, Tijmen Blankevoort, and Max Welling. Data-free quantization through weight equalization and bias correction. In *Proceedings of the IEEE/CVF International Conference on Computer Vision (ICCV)*, October 2019. 1, 2, 4, 5, 6, 8
- [39] Sharan Narang, Erich Elsen, Gregory Diamos, and Shubho Sengupta. Exploring sparsity in recurrent neural networks, 2017. 1
- [40] Adam Paszke, Sam Gross, Francisco Massa, Adam Lerer, James Bradbury, Gregory Chanan, Trevor Killeen, Zeming Lin, Natalia Gimelshein, Luca Antiga, Alban Desmaison, Andreas Kopf, Edward Yang, Zachary DeVito, Martin Raison, Alykhan Tejani, Sasank Chilamkurthy, Benoit Steiner, Lu Fang, Junjie Bai, and Soumith Chintala. Pytorch: An imperative style, high-performance deep learning library. In H. Wallach, H. Larochelle, A. Beygelzimer, F. d'Alché-Buc, E. Fox, and R. Garnett, editors, *Advances in Neural Information Processing Systems 32*, pages 8024–8035. Curran Associates, Inc., 2019. 3, 6
- [41] Mohammad Rastegari, Vicente Ordonez, Joseph Redmon, and Ali Farhadi. Xnor-net: Imagenet classification using binary convolutional neural networks. In *European Conference on Computer Vision*, pages 525–542. Springer, 2016. 1, 2
- [42] Joseph Redmon and Ali Farhadi. Yolo9000: Better, faster, stronger. In *Computer Vision and Pattern Recognition (CVPR), 2017 IEEE Conference on*, pages 6517–6525. IEEE, 2017. 1
- [43] Mark Sandler, Andrew G. Howard, Menglong Zhu, Andrey Zhmoginov, and Liang-Chieh Chen. Inverted residuals and linear bottlenecks: Mobile networks for classification, detection and segmentation. *CoRR*, abs/1801.04381, 2018. 6, 7
- [44] Suraj Srinivas and R. Venkatesh Babu. Data-free parameter pruning for deep neural networks. *CoRR*, abs/1507.06149, 2015. 2
- [45] X. Suau, u. Zappella, and N. Apostoloff. Filter distillation for network compression. In *2020 IEEE Winter Conference on Applications of Computer Vision (WACV)*, pages 3129–3138, 2020. 2
- [46] Mingxing Tan and Quoc V. Le. Efficientnet: Rethinking model scaling for convolutional neural networks. *CoRR*, abs/1905.11946, 2019. 1, 5, 6, 7, 8
- [47] Mitchell Wortsman, Ali Farhadi, and Mohammad Rastegari. Discovering neural wirings. In H. Wallach, H. Larochelle, A. Beygelzimer, F. d'Alché-Buc, E. Fox, and R. Garnett, editors, *Advances in Neural Information Processing Systems*, volume 32, pages 2684–2694. Curran Associates, Inc., 2019. 1
- [48] Hao Wu, Patrick Judd, Xiaojie Zhang, Mikhail Isaev, and Paulius Micikevicius. Integer quantization for deep learning inference: Principles and empirical evaluation, 2020. 2
- [49] Shoukai Xu, Haokun Li, Bohan Zhuang, Jing Liu, Jiezhong Cao, Chuangrun Liang, and Mingkui Tan. Generative low-bitwidth data free quantization, 2020. 2
- [50] Yukuan Yang, Shuang Wu, Lei Deng, Tianyi Yan, Yuan Xie, and Guoqi Li. Training high-performance and large-scale deep neural networks with full 8-bit integers, 2019. 2
- [51] Hongxu Yin, Pavlo Molchanov, Jose M. Alvarez, Zhizhong Li, Arun Mallya, Derek Hoiem, Niraj K Jha, and Jan Kautz. Dreaming to distill: Data-free knowledge transfer via deep-inversion. In *The IEEE/CVF Conf. Computer Vision and Pattern Recognition (CVPR)*, 2020. 1, 2, 3, 7, 8